

# NLRP3 Blockade Suppresses Pro-Inflammatory and Pro-Angiogenic Cytokine Secretion in Diabetic Retinopathy

This article was published in the following Dove Press journal:  
*Diabetes, Metabolic Syndrome and Obesity: Targets and Therapy*

Guangrui Chai<sup>1</sup>  
Shu Liu<sup>2</sup>  
Hongwei Yang<sup>1</sup>  
Guoqiang Du<sup>3</sup>  
Xiaolong Chen<sup>1</sup>

<sup>1</sup>Department of Ophthalmology, Shengjing Hospital of China Medical University, Shenyang, Liaoning, People's Republic of China; <sup>2</sup>Department of Geratology, The First Affiliated Hospital of China Medical University, Shenyang, Liaoning, People's Republic of China; <sup>3</sup>Department of Otolaryngology, Qingdao Municipal Hospital, Qingdao, Shandong, People's Republic of China

**Background:** Inflammation and angiogenesis are the two dominant mechanisms of diabetic retinopathy (DR), which act more as mutual pathways rather than individual processes. However, the underlying mechanism of their interactions is still unclear. Here, we explored the potential crossing points between these pathways and the targeted therapeutic method in rats with DR.

**Materials and Methods:** Sprague–Dawley rats were randomly assigned to four groups: normal control group, streptozocin (STZ)-induced diabetes mellitus (DM) group, DM+shNC (non-specific negative control shRNA) group, and DM+shNLRP3 group. Silencing the NLR family pyrin domain containing 3 (NLRP3) protein was performed by intravitreal injections of *NLRP3*-targeted shRNA (shNLRP3) for rats in the DM+shNLRP3 group. All the rats' retinas were collected for further morphological examination and pro-inflammatory and pro-angiogenic cytokine detection. Human retinal endothelial cells (HRECs) were also employed to explore the underlying mechanism.

**Results:** *NLRP3*-targeted shRNA given by intravitreal injection effectively alleviated the retinal histopathological changes in STZ-induced diabetic rats, which reduced the activation of the NLRP3 inflammasome and suppressed the expressions of hypoxia-inducible factor-1 $\alpha$  (HIF-1 $\alpha$ ), vascular endothelial growth factor (VEGF), and inflammatory cytokines in diabetic rats' retinas. In HRECs, *NLRP3* over-expressing plasmid evoked an increase in pro-inflammatory cytokines and VEGF. In addition, YC-1, a HIF-1 $\alpha$  inhibitor, could reverse the *NLRP3* over-expression-induced VEGF production but not the pro-inflammatory cytokine expressions.

**Conclusion:** Our results suggest *NLRP3* inflammasome as the potential cross-point between inflammation and pro-angiogenesis in DR and support the effectiveness of *NLRP3*-targeted shRNA administrated by intravitreal injection in animal models of DR. The protective effect of *NLRP3*-targeted shRNA may stem from the inhibition of both pro-inflammatory cytokines and HIF-1 $\alpha$ /VEGF axis.

**Keywords:** *NLRP3* inflammasome, inflammation, angiogenesis, VEGF, diabetic retinopathy

## Introduction

Due to lifestyle changes in modern society, more than 8.8% of the global population have suffered from diabetes mellitus (DM).<sup>1</sup> Diabetic retinopathy (DR), one of the most prevalent and serious microvascular complications of DM, remains the leading cause of irreversible blindness in working-age people and its incidence continues unabated.<sup>2</sup> Unfortunately, there is still a lack of early-stage therapeutic interventions. Thus, a better understanding of the molecular origins of DR and novel diagnostic and targeted therapeutic approaches are warranted. Morphologically, DR results in the

Correspondence: Xiaolong Chen  
Email chenxl@sj-hospital.org

decrease of retinal thickness and loss of ganglion cells, endothelial cells, and pericytes. In terms of mechanism, retinal inflammation and neovascularization are generally accepted as influencing factors in the progression of DR.<sup>3</sup> Persistent hyperglycemia induces hemodynamic and metabolic abnormalities, which evoke the local inflammatory response by stimulating the secretion of pro-inflammatory factors such as interleukin (IL), C-reactive protein (CRP), and tumor necrosis factor (TNF). Furthermore, these result in a vicious cycle due to the loss of endothelial cells induced by excessive inflammation, an imbalance of vascular permeability, microvascular occlusions, the release of ischemic signals, VEGF-related neovascularization, and presence of fragile and hemorrhage-prone neovascularized vessels which may enhance ischemia and inflammation. Though more evidence emphasized the interconnection between vascular inflammation and neovascularization,<sup>4</sup> an understanding of the detailed underlying mechanisms is still deficient.

Sustainable low-grade inflammation induced by continuous hyperglycemia is considered the basis of the development of DR. Recently, this low-grade inflammatory response was partially attributed to the dysfunction of the innate immune system under high glucose conditions.<sup>5,6</sup>

Inflammasomes were regarded as an important component of innate immunity, among which the NLR family, pyrin domain containing 3 (NLRP3) inflammasome received the most concern. NLRP3 inflammasome is a multi-protein scaffold which is composed of three parts including NLRP3, apoptosis-associated speck-like protein containing a CARD (ASC), and a caspase-1 precursor. It can be activated by various exogenous pathogen associated molecular patterns (PAMPs) or endogenous damage associated molecular patterns (DAMPs) and then provides a molecular platform for the maturation of caspase-1, IL-1 $\beta$ , and IL-18.<sup>7</sup> NLRP3 inflammasome was reported to be involved in various malignant tumors,<sup>8</sup> autoimmune diseases,<sup>9</sup> ischemia reperfusion injury,<sup>10</sup> and many other infectious diseases. In regards to ocular diseases, the activation of NLRP3 inflammasome has been observed in acute glaucoma,<sup>11</sup> ocular infections, xerophthalmia,<sup>12</sup> and macular degeneration,<sup>13</sup> as well as diabetic retinopathy.<sup>14</sup> The damage to cells or tissues by metabolic abnormalities will cause the release of PAMPs and DAMPs. The released PAMPs and DAMPs induced by hyperglycemic injury can further up-regulate NLRP3 inflammasome, which consequently increases the secretion of IL-1 $\beta$  in retinal pigmented epithelial (RPE) cells in high-glucose media.<sup>15</sup> Furthermore, secreted IL-1 $\beta$  and IL-18 mediate the

inflammatory cascade reaction. Blocking NLRP3 inflammasome activation significantly reduced IL-1 $\beta$  in retinal endothelial cells.<sup>16</sup> Nevertheless, it is still unclear about the concrete role of NLRP3 inflammasome in the pathogenic mechanism and the therapeutic efficacy of NLRP3 inflammasome inhibition in the *in vivo* models of DR.

In addition to inflammation, pathologic neovascularization plays another key role in DR. Recently, it been indicated that NLRP3 inflammasome activation may also participate in this process but the specific signaling pathway is blurred.<sup>14</sup> Hypoxia-inducible factor 1 $\alpha$  (HIF-1 $\alpha$ ), vascular endothelial growth factor (VEGF), soluble intercellular adhesion molecule-1 (sICAM-1), platelet endothelial cell adhesion molecule-1 (PECAM-1/CD31), and von Willebrand factor (VWF) are the classic cytokines related to neovascularization in DR. An anti-VEGF reagent has emerged, but its clinical application is limited due to the high price and short maintenance time. Novel treatment methods are urgently needed to solve this problem.

Therefore, we designed this study to investigate the relationship between NLRP3 inflammasome and the secretion of pro-inflammatory and pro-angiogenic cytokines in DR, aiming to explore the potential interlink between inflammatory reactions and angiogenesis. All in all, we aim to improve the understanding of the pathogenesis of DR and to search for more effective preventive and therapeutic targets.

## Materials and Methods

### Experimental Animals

We purchased male Sprague–Dawley rats (SPF level, 8 weeks old, weight: 200–220 g) from the Beijing Huafukang Biotechnology Co., Ltd. They were all raised in the research center of Shengjing Hospital of China Medical University (room temperature: 18–22°C, humidity: 50–60%). All animal protocols were in adherence to the regulations on the administration of experimental animals issued by the National Science and Technology Commission. All the animal-related manipulations were approved by the Ethical Committee of China Medical University (No.2016PS229K) prior to implementation.

### Construction of shRNAs Targeting NLRP3 and Intravitreal Injection of shRNAs

The non-specific negative control shRNA (shNC) and specific shRNA targeting NLRP3 were designed and provided by GenePharma (Shanghai, China). The sequences of shRNA targeting NLRP3 are sense 5'-GATCCCGTTAGAAAC

ACTTCAAGAACTCGAGTTCTTGAAGTGTTCCTAAC-GCTTTTTGGAT-3', antisense 5'-AGCTATCCAAAAAGTTAGAAACACTTCAAGAACTCGAGTTCTTGAAGTGTTCCTAACGCGG. The sequences of shNC are sense 5'-GATCCCACAGTGTAACTGCAGAACTCGAGTTCTG-CAGGTTACTGTGGTTTTTGGAT-3', antisense 5'-AGCTATCCAAAAACAGTGTAACTGCAGAACTCGAGTTCTGCAGTTACTGTGGGG. Before use, the resultant shRNA was centrifuged at 5000×g for 10 min. Then, 50µg shRNA was dissolved in 5µL DEPC-treated water to make the shRNA solution (10µg/µL). In addition, 0.55 µL Lipofectamine 2000 (24 µg) was diluted with 0.45 µL DEPC-treated water to make the Lipofectamine 2000 solution. According to the instructions, we mixed 1µL shRNA solution (10µg/µL) and 1µL Lipofectamine 2000 solution (24µg/µL) at room temperature 30 min before intravitreal injection. Thereafter, this shRNA mixture was used for intravitreal injections. Intravitreal injections were carried out according to our previous study.<sup>17</sup> Briefly, after mydriasis with 0.5% tropicamide-phenylephrine eyedrops (Santen, Tokyo, Japan) and topical anesthesia with 0.4% oxybuprocaine hydrochloride (Santen, Tokyo, Japan), a microsyringe was applied for insertion into the vitreous cavity of both eyes under a surgical microscope while avoiding lens damage. After injection, rats received ofloxacin eye drops (Santen, Tokyo, Japan) for infection prevention.

## Animal Grouping and Interventions

Forty-four Sprague–Dawley rats were assigned to four groups at random. Respectively, the four groups were named as a normal control group (eight rats), DM group (twelve rats), DM+shNC (non-specific negative control shRNA) group (twelve rats), and DM+shNLRP3 group (twelve rats). Except for the eight rats of the normal control group, diabetes was induced in all rats with freshly prepared streptozocin (STZ) solution in citrate buffer (pH 4.5). The rats were given a single intraperitoneal injection of STZ with a dosage of 60 mg/kg body weight. The diabetic model was considered to be successful since rats had a random blood glucose  $\geq 16.7$  mmol/L (measured with blood samples gained from the caudal vein) more than 72 hours after STZ injection. Besides the blood glucose test at 72 hours after the injection of STZ, all the rats were detected for blood glucose once a week until the end of the study. At 4, 8 and 12 weeks after intraperitoneal injection of STZ, we made intravitreal injections for rats as follows: 1) normal control group and DM group: 2 µL sterilized saline; 2) DM+shNC (NLRP3): 2 µL non-

specific shNC; 3) DM+shNLRP3: 2 µL shNLRP3. During the 16 weeks studying period, four rats (one in DM group, one in DM+shNC group, and two in DM+shNLRP3 group) showed a random blood glucose  $< 16.7$  mmol/L and were excluded from further research. Eight rats (three in DM group, three in DM+shNC group and two in DM+shNLRP3 group) died of infections and there were eight rats left per group at the end-point of our research. At 16 weeks after STZ injection, all the remaining rats were euthanized and their eyeballs were preserved for further detection.

## Histopathological Examination of Retinas

For further histo-morphological examinations, we fixed the rats' eyeballs (right eyes) with 4% paraformaldehyde at 4°C for 4 h. After fixation, the rats' eyeballs were gently taken out and further embedded with paraffin. Retinal sections (4 µm in thickness) were acquired at 1 mm next to the temporal margin of the optic disc followed by H&E staining for pathological observations using a light microscope ( $\times 40$ , Eclipse Ci, Nikon). In order to make some quantitative comparisons of the retina changes among different groups, we used NIS-Elements Basic Research Software (version 4.30, Nikon) to randomly take five microphotographs for each tissue section and used Image J Software (version 1.8.0, National Institutes of Health) to perform related measurements. The measured parameters mainly concerned retinal thickness and amount of ganglion cells in the ganglion cell layer (GCL). The retinal thickness was reflected as the thickness of the inner nuclear layer (INL) and outer nuclear layer (ONL) as well as the thickness between the inner limiting membrane (ILM) and the outer limiting membrane (OLM).

## ELISA Detection of Cytokines in Retinas

After peeling off, the retinas (without retinal pigment epithelium) of eight rats (left eye) in each group were mixed with ice-cold buffer (0.9% saline solution containing 1 µg/L protease inhibitor) to make 100 g/L tissue homogenate. Next, we centrifugated the homogenate at 4270×g for 20 min and collected the supernatant. The concentrations of VEGF and sICAM-1 in the supernatant were measured using specific ELISA kits (VEGF ELISA kit for rats, BOSTER Biological Technology Co. Ltd, Wuhan, China; sICAM-1 ELISA kit for rats, Ruishuo Biotechnology Co., Ltd, Shanghai, China). Moreover, the inflammatory cytokines such as IL-1 $\beta$  and IL-18 (Dakewe Biotech Co., Ltd, Shenzhen, China), TNF- $\alpha$  and IL-6

(Jiancheng Biotech Co., Ltd, Nanjing, China) were also detected according to the specific kits' instructions.

## Human Retinal Endothelial Cell Culture and Treatment

Human retinal endothelial cells (HRECs) were purchased from the Cellular Institute of China Scientific Academy. After recovery and passage, cells were cultured and separated into five groups, named LG group, HG group, HG+ vector control group, HG+ pcDNA3-N-FlagNLRP3 group, and HG + pcDNA3-N-FlagNLRP3+YC-1 group. In the LG group, cells were cultured in system media DMEM (BIOIND, Israel) containing 10% fetal bovine serum and 1% penicillin–streptomycin with normal glucose (5.5 mM/L). Cells in the other four groups were cultured in DMEM (BIOIND, Israel) containing 10% fetal bovine serum and 1% penicillin–streptomycin with high glucose (30 mM/L). After being seeded into the 24-well culture plate at a uniform density of  $4 \times 10^5$  cells/well the day before transfection, cells in the HG+ vector control group were transfected with empty vector control of pcDNA3-N-FlagNLRP3 and cells in the HG+ pcDNA3-N-FlagNLRP3 group and the HG+ pcDNA3-N-FlagNLRP3+YC-1 group were transfected with plasmid pcDNA3-N-FlagNLRP3 (#75,127, Addgene, USA) according to the Lipofectamine 2000 transfection reagent's (Thermo Fisher Scientific, USA) instructions. Briefly, 0.8  $\mu$ g DNA was added into 50  $\mu$ L serum-free DMEM media. Then, 2  $\mu$ L Lipofectamine 2000 was diluted with 50  $\mu$ L serum-free DMEM and left at room temperature for 5 min. After that, the diluted DNA and Lipofectamine 2000 were gently mixed and placed for 20 min at room temperature. Next, 100  $\mu$ L DNA/lipofectamine was added per well. The mixtures of transfection reagents, vector or plasmid, and cells were incubated at 37°C and 5% CO<sub>2</sub> (V/V) for 6 hours then the media was replaced with their primary culture media with high glucose (30 mM/L). After that, YC-1 (an inhibitor of HIF-1 $\alpha$ , 1.0  $\mu$ g/mL, Calbiochem, USA)<sup>18</sup> was added in the media of the HG+ pcDNA3-N-FlagNLRP3+YC-1 group. All the cells were cultured for another 48 hours and the supernatants were collected for ELISA assay of IL-1 $\beta$ , IL-18, IL-6, and VEGF.

## Real-Time PCR Assay

Total RNA was isolated from the retina samples with Trizol reagent (Thermo Fisher Scientific, Inc.) and reverse transcribed into cDNA (Takara Bio, Tokyo, Japan) following the manufacturer's instructions. The amplification was implemented

with SYBR Green PCR Master Mix (Takara Bio, Japan) in a total volume of 20  $\mu$ L with an Applied Biosystems 7500 Fast Real-Time PCR system by denaturing at 95°C for 30 s, and 40 cycles of 95°C for 3 s, 60°C for 30 s, and 95°C for 5 s. The mRNA expression levels of *Nlrp3*, *ASC*, *caspase-1*, *IL-1 $\beta$* , *HIF-1 $\alpha$* , *Vegf*, *Pecam-1*, *Vwf*, and  $\beta$ -actin were tested and their primer sequences are listed in Table 1. The values were normalized by those in the normal control group.

## Western Blot Analysis

We extracted total protein from pulverized retinal samples and cell culture lysates which were mixed with RIPA buffer (Thermo Fisher Scientific, Inc.) with 1% PMSF. The concentration of total protein was tested with the BCA Protein Quantification Kit (Beyotime Biotechnology, Shanghai, China). After thermal denaturation (at 100°C for 10 min), the protein samples were run on 10% or 12% SDS-PAGE gels. Thereafter, the separated protein bands were transferred to PVDF membranes which were further blocked with 5% skim milk powder for two hours at room temperature. To identify specific protein expression, the membranes were incubated with specific primary antibodies (anti-NLRP3: 1:500, Abcam; anti-ASC: 1:500, Bioss, Beijing, China; anti-caspase-1: 1:1000, Bioss; anti-IL-1 $\beta$ : 1:1000,

**Table 1** Primer Sequences

Gene	Primer Sequences (5'-3')
<i>Nlrp3</i>	Forward TCTGACCTCTGTGCTCAAACCAAC Reverse TGAGGTGAGGCTGCAGTTGTCTAAT
<i>ASC</i>	Forward GCACAGCCAGAACAGAACAT Reverse AGCACATTGCCATACAGAGC
<i>caspase-1</i>	Forward TGCAGCACAGACTTTCAACA Reverse CTGCAGCAGCAACTTCATTT
<i>IL-1<math>\beta</math></i>	Forward TCTGTGACTCGTGGGATGAT Reverse TTGTTGTTTCATCTCGAAGCC
<i>HIF-1<math>\alpha</math></i>	Forward TTTGCTGAAGACACAGAAGCAAAGA Reverse TTGAGGACTTGCCTTTCAGG
<i>Vegf</i>	Forward GCTCCATTCTGTAGGCTCTG Reverse CCAGAGCACAGACTCCCTGGCT
<i>Pecam-1</i>	Forward AACAGTGTGACATGAAGAGCC Reverse TGAAAACAGCACGTCATCCTT
<i>Vwf</i>	Forward CCGATGCAGCCTTTTCGGA Reverse TCCCCAAGATACACGGAGAGG
$\beta$ -actin	Forward AGCGCAAGTACTCTGTGTGG Reverse AACAGTCCGCCTAGAAGCAT

Bioss; anti-HIF-1 $\alpha$ : 1:500, Bioss; anti-VEGF: 1:500, Bioss; anti- $\beta$ -actin: 1:1000, Bioss) at 4°C overnight for sufficient reaction. Then, horseradish peroxidase labeled second antibodies (1:10,000, ZSGB-BIO, Beijing, China) were used to form the protein–antibody complexes that were inspected with the enhanced chemiluminescent assay. Protein band intensities were normalized to  $\beta$ -actin.

## Wound Healing and Tube Formation Assays

Wound healing and tube formation assays were employed to investigate the migration and angiogenic capability of HRECs in the five groups mentioned above. Cells of the five groups (LG group, HG group, HG+ vector control group, HG+ pcDNA3-N-FlagNLRP3 group, and HG+ pcDNA3-N-FlagNLRP3+YC-1 group) were seeded in the 24-well plates at a uniform density of  $4 \times 10^5$  cells/well. After cells were cultured to achieve 100% confluence, we used a 10  $\mu$ L pipette tip to create scratches on the monolayer cells in each well and washed the scratched cells with PBS. Images were taken at  $\times 100$  magnification immediately after scratching (0 h) and 24 hours (24 h) after cells were cultured with 500  $\mu$ L serum-free media with mitomycin C (5  $\mu$ g/m) to inhibit cell proliferation. Image J software (version 1.8.0) was utilized to calculate the area of the remaining scratch.

As for the tube formation test, we thawed the Matrigel at 4°C overnight before use. After that, 50  $\mu$ L Matrigel/well was placed in a cooled 96-well plate which was further incubated at 37°C for 30 min. When the Matrigel became solid, HRECs of the five groups were seeded at a density of  $2 \times 10^4$  cells per well. After 4 hours' incubation (37°C, 5% CO<sub>2</sub>, and 95% air), images were taken (at  $\times 200$  magnification) for further evaluation of the number of junctions, the number of branches and the total branching length with Image J software.

## Statistical Analysis

All the numerical data were present as mean $\pm$ SD and statistically analyzed with GraphPad Prism 7.0 (GraphPad Software Inc., USA). For multiple comparison among groups, we performed one-way analysis of variance (ANOVA), and  $p < 0.05$  was determined as statistically significant.

## Results

### Down-Regulated Expression of NLRP3 Can Alleviate Histopathological Changes in Retinas of STZ-Induced Diabetic Rats

Rats' retinas were examined with H&E staining to observe the histopathological alterations in different

groups. In the normal control group, the thickness of retinas was normal. The retinal cells were arranged in the INL and ONL in an orderly manner with uniform density, and there were sufficient ganglion cells in GCL (Figure 1A Normal). However, diabetes induced morphological changes of retinas which mainly manifested as decreased retinal thickness, marked reduction of cell numbers in INL, ONL and GCL, and irregular and loose cell arrangement in the DM group (Figure 1A DM). Similar alterations could be observed in the non-specific shRNA negative control group (Figure 1A DM+shNC). It is noteworthy that down-regulating the expression of NLRP3 by intravitreal injections with a specific shRNA (shNLRP3) could significantly reverse the high blood glucose-induced retinal damage, leading to greater retinal thickness and more uniformly distributed cells in INL and ONL compared to those in the DM group (Figure 1A DM+shNLRP3). In the DM+shNLRP3 group, the thickness between ILM and OLM was  $199 \pm 66$   $\mu$ m while those values in the DM group and DM+shNC group were  $123 \pm 45$   $\mu$ m and  $128 \pm 52$   $\mu$ m ( $*p < 0.05$ ) (Figure 1B). A similar observation could be made in the greater thickness of INL and ONL in the DM+shNLRP3 group as compared to the DM group and the DM+shNC group ( $*p < 0.05$ ) (Figure 1C, D). Loss of ganglion cells in GCL is a typical feature of DR. In this study, the DM+shNLRP3 group showed a markedly increased amount of ganglion cells ( $128.6 \pm 14.26$  per  $\text{mm}^2$ ) compared with the DM group ( $62.88 \pm 16.40$  per  $\text{mm}^2$ ) and the DM+shNC group ( $64.25 \pm 16.70$  per  $\text{mm}^2$ ) in regards to the ganglion cell count in GCL ( $**p < 0.01$ ) (Figure 1E). Overall, the DM+shNLRP3 group, in comparison to the DM group and the DM+shNC group, showed greater thickness between ILM and OLM, greater thickness of INL and ONL, and more ganglion cells in GCL. In addition, the blood glucose levels of the rats during the study period were shown for reference (Figure 1F).

### Silencing of NLRP3 Reduces the Expressions of Inflammatory Cytokines and VEGF in the Retinas of STZ-Induced Diabetic Rats

To explore the potential reason for the protective effect of NLRP3 knock-down, we measured the levels of pro-inflammatory and pro-angiogenic cytokines in the supernatant of the retinal homogenate. Compared to those in the normal control group, the levels of IL-1 $\beta$ , IL-18,

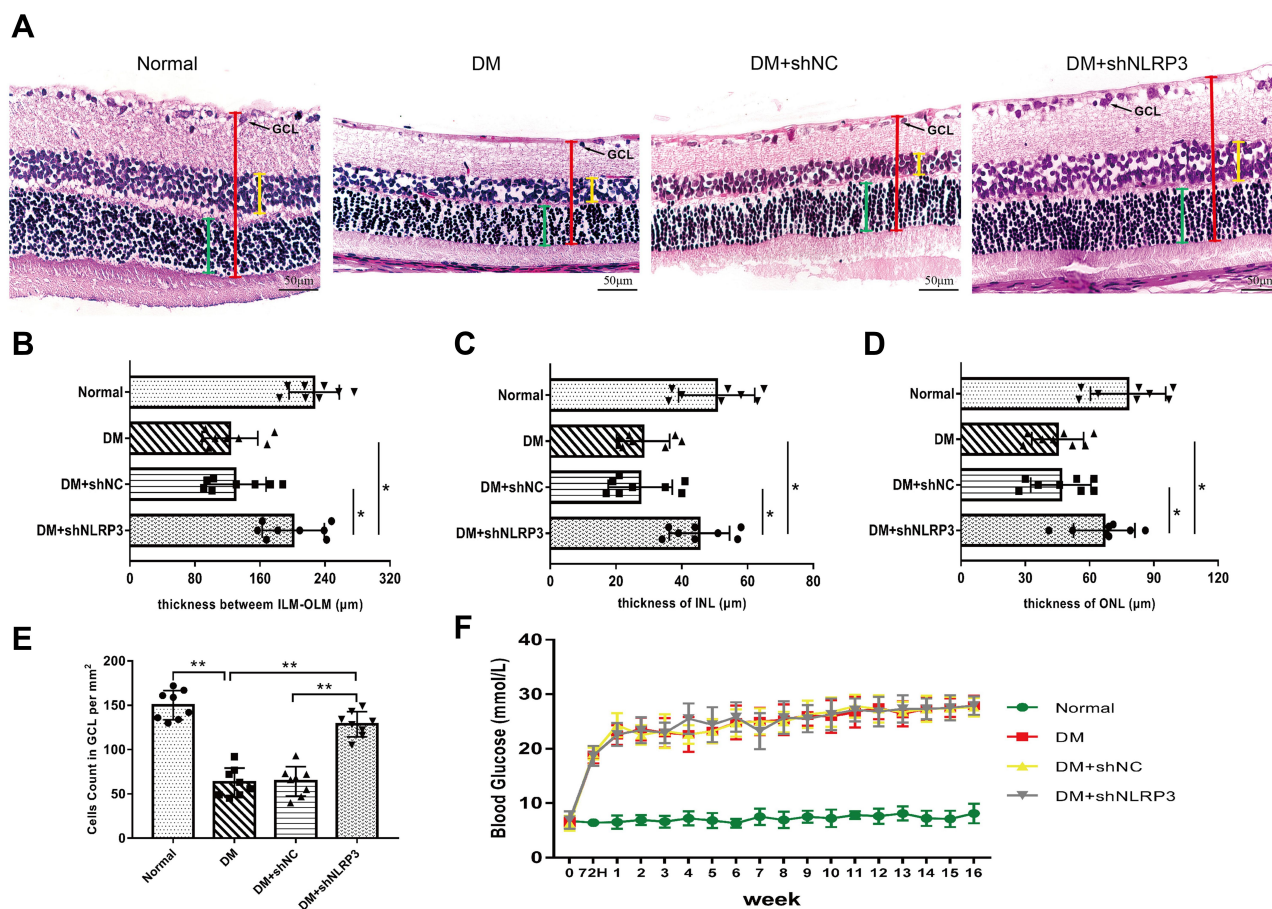


**Figure 1** Down-regulating retinal expression of *NLRP3* with a specific shRNA can alleviate the histopathological changes of retinas in STZ-induced diabetic rats. **(A)** Histopathological changes of retinas examined with hematoxylin-eosin staining ( $\times 40$ , scale bar  $50 \mu\text{m}$ ). Retinal cells were arranged in an orderly manner in each layer and revealed uniform density in the normal control group (Normal). In contrast, the GCL was irregularly and loosely arranged in the DM and DM+shNC group. Inhibiting *NLRP3* expression with shNLRP3 partially reversed the high-glucose-induced damages (DM+shNLRP3). **(B–D)** In the DM+shNLRP3 group, the thickness between ILM and OLM (red line segment), the thickness of INL (yellow line segment) and ONL (green line segment) were greater than those values in the DM group and DM+shNC group ( $*p < 0.05$ ). **(E)** DM+shNLRP3 group showed a markedly increased ganglion cell number in GCL compared with the DM group and DM+shNC group ( $**p < 0.01$ ). **(F)** The blood glucose status of the rats during the study period. Data are expressed as mean  $\pm$  SD,  $n = 8$  biological replicates.

**Abbreviations:** *NLRP3*, NLR family, pyrin domain containing 3; STZ, streptozotocin; DM, diabetes mellitus; ILM, inner limiting membrane; OLM, outer limiting membrane; INL, inner nuclear layer; ONL, outer nuclear layer; shNC, negative control shRNA of shNLRP3.

IL-6, and TNF- $\alpha$  were significantly elevated in the DM group and the DM+shNC group (Figure 2A–D). As well, there was no statistical difference in the levels between these two groups ( $p > 0.05$ ). Reducing the expression of *NLRP3* with a targeted shRNA inhibited the abnormally increased levels of these inflammatory factors (Figure 2A–D). The striking aspect of these results was that VEGF and sICAM-1 expressions showed a simultaneous decrease with the down-regulation of *NLRP3* (Figure 2E, F). What stands out here was that the expression levels of VEGF were positively correlated with those of IL-1 $\beta$  and IL-6 according to the results of the correlational analysis (Figure 2G, H).

## Silencing of *NLRP3* Inhibits Not Only the Activation of the *NLRP3* Inflammasome But Also HIF-1 $\alpha$ and VEGF Expressions in the Retinas of STZ-Induced Diabetic Rats

Consequently, we made a further exploration of the underlying mechanism of the above changes in the levels of pro-inflammatory and pro-angiogenic cytokines. As can be seen from the graph, the mRNA and protein levels of *NLRP3* inflammasome related indexes (*NLRP3*, ASC, caspase-1, and IL-1 $\beta$ ) dramatically increased in the DM group as compared with those in the normal control group (Figure 3A–C). Intervention with shNLRP3 not only successfully inhibited the expression of *NLRP3*, but also caused a clear

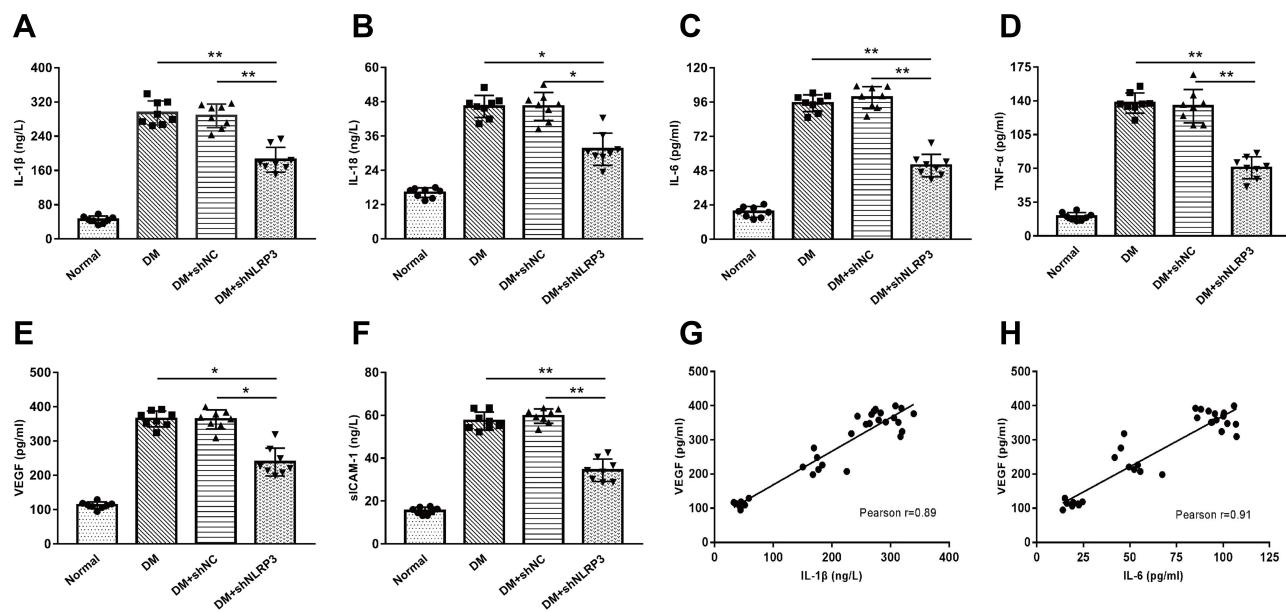


**Figure 2** Silencing of *NLRP3* reduces the expressions of inflammatory cytokines and VEGF in the retinas of STZ-induced diabetic rats. (A–D) Compared to those in the normal control group, the levels of IL-1 $\beta$ , IL-18, IL-6, and TNF- $\alpha$  were significantly elevated in the DM and DM+shNC group. There was no statistical difference between these two groups ( $p>0.05$ ). Reducing the expression of *NLRP3* with a targeted shRNA inhibited the abnormally increased levels of these inflammatory factors ( $*p<0.05$ ;  $**p<0.01$ ). (E–F) The levels of VEGF and sICAM-1 increased in the DM and DM+shNC group, while shNLRP3 partially reversed these increases ( $*p<0.05$ ;  $**p<0.01$ ). (G–H) The expression level of VEGF was positively correlated with those of IL-1 $\beta$  and IL-6 in the rats' retinas. Data are shown as mean $\pm$ SD,  $n=8$  biological replicates.

**Abbreviations:** IL-1 $\beta$ , interleukin-1 $\beta$ ; IL-18, interleukin-18; IL-6, interleukin-6; TNF- $\alpha$ , tumor necrosis factor- $\alpha$ ; DM, diabetes mellitus; shNC, negative control shRNA of shNLRP3; VEGF, vascular endothelial growth factor; sICAM-1, soluble intercellular adhesion molecule-1.

trend of decreasing *NLRP3* inflammasome expression and activation. Compared to those in the DM group, there were significant declines in the mRNA and protein levels of the *NLRP3* inflammasome related indexes including *NLRP3*, ASC, caspase-1, and IL-1 $\beta$  in the DM+shNLRP3 group ( $**p<0.01$  for *NLRP3* and IL-1 $\beta$ ;  $*p<0.05$  for ASC and caspase-1) (Figure 3A–C). Simultaneously, the mRNA and protein levels of HIF-1 $\alpha$  and VEGF were elevated in the high glucose environment which can be seen in the DM and DM+shNC groups (Figure 3A–C). *NLRP3* knock-down remarkably reversed the high glucose induced HIF-1 $\alpha$  and VEGF over-expression in the DM+shNLRP3 group ( $**p<0.01$ ) (Figure 3A–C).

### *NLRP3* Over-Expression Promotes Secretion of Pro-Inflammatory and Pro-Angiogenic Cytokines in HRECs Cultured in High-Glucose Media and HIF-1 $\alpha$ Inhibitor Can Reverse *NLRP3*-Induced VEGF Production

Based on the previous findings, we used HRECs to discover the possible interaction pathway that might be influenced by the *NLRP3* inflammasome between inflammatory factors

and pro-angiogenic VEGF. A plasmid over-expressing *NLRP3* was constructed and transfected into HRECs. The Western blot assay of *NLRP3* proved the validity of the over-expressing plasmid pcDNA3-N-FlagNLRP3, since the *NLRP3* expression in the HG+ pcDNA3-N-FlagNLRP3 group and the HG+ pcDNA3-N-FlagNLRP3+YC-1 group was greater by 3.11 and 3.18 folds compared to that in the HG group, respectively (Figure 4A). In the high-glucose culture media, cells transfected with *NLRP3* over-expressing plasmid produced significantly higher levels of IL-1 $\beta$ , IL-18 and IL-6 compared to the HG and HG+vector control group ( $p<0.01$ ,  $p<0.001$ , and  $p<0.01$ , respectively) (Figure 4B–D). In the HG+ pcDNA3-N-FlagNLRP3+YC-1 group, treatment with YC-1, an inhibitor of HIF-1 $\alpha$ , did not affect the increased production of pro-inflammatory IL-1 $\beta$  and IL-18 (Figure 4B, C). There was no statistically significant decrease in IL-6 level in the HG+ pcDNA3-N-FlagNLRP3+YC-1 group as compared with that in the HG+ pcDNA3-N-FlagNLRP3 group (Figure 4D).

Meanwhile, the high-glucose condition could stimulate the expressions of HIF-1 $\alpha$ , VEGF, PECAM-1, and VWF in HRECs. This stimulatory effect was significantly enhanced in the presence of *NLRP3* over-expressing plasmid, which mainly manifested as elevated expressions of

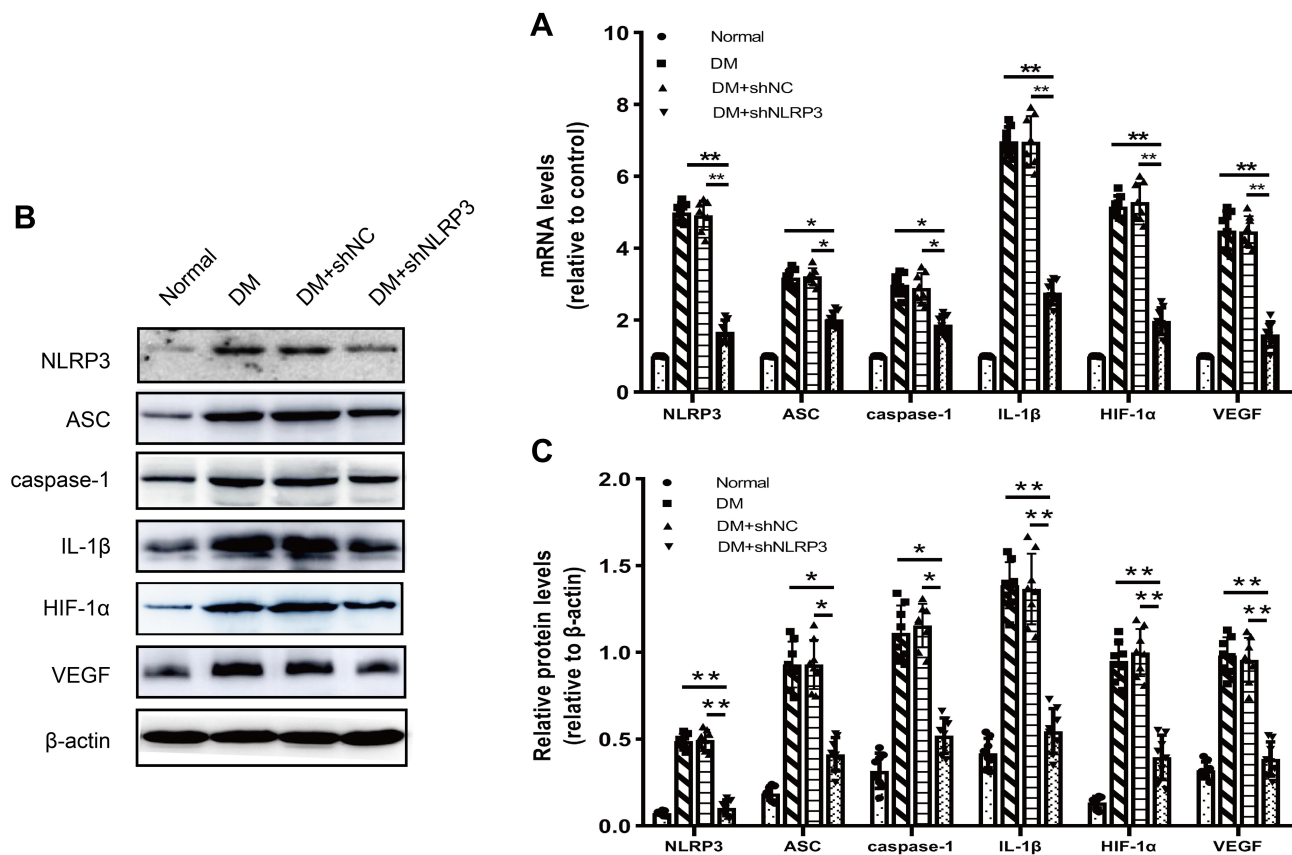


**Figure 3** Silencing of *NLRP3* inhibits the activation of the *NLRP3* inflammasome as well as expressions of *HIF-1α* and *VEGF* in the retinas of STZ-induced diabetic rats. **(A)** mRNA levels of *NLRP3* inflammasome related indexes (*NLRP3*, *ASC*, *caspase-1*, and *IL-1β*), *HIF-1α* and *VEGF* dramatically increased in the DM group as compared with those in the normal control group ( $*p<0.05$ ;  $**p<0.01$ ). Intervention with sh*NLRP3* not only successfully inhibited the expression of *NLRP3*, but also caused a clear trend of decreasing *NLRP3* inflammasome activation and *HIF-1α*/*VEGF* expressions. **(B–C)** Compared to those in the DM group, there were significant declines in the protein levels of *NLRP3* inflammasome related indexes in the DM+sh*NLRP3* group, especially *IL-1β* ( $*p<0.05$ ;  $**p<0.01$ ). Simultaneously, protein levels of *HIF-1α* and *VEGF* in each group showed a similar change in trends. **(B)** is a representative image of Western blot assay. Data are expressed as mean $\pm$ SD, n=8 biological replicates.

**Abbreviations:** *ASC*, apoptosis-associated speck-like protein containing a CARD; *caspase-1*, cysteinyl aspartate specific proteinase-1; *IL-1β*, interleukin-1β; *HIF-1α*, hypoxia inducible factor-1α; *VEGF*, vascular endothelial growth factor.

*HIF-1α*, *VEGF*, *PECAM-1*, and *VWF* in the HG+ pcDNA3-N-Flag*NLRP3* group in contrast to the HG and HG+vector control group ( $**p<0.01$ ) (Figure 4A, E–G). Inhibiting *HIF-1α* with *YC-1* can obviously reverse *NLRP3*-induced *PECAM-1*, *VWF*, and *VEGF* production (Figure 4E–G). To eventually reinforce *NLRP3*'s role on the side of the angiogenic effect, we performed wound healing and tube formation assays. Similarly, the high-glucose condition could stimulate cells' migration and capillary forming ability, which was significantly enhanced in the presence of *NLRP3* over-expressing plasmid (Figure 4H–L). *HIF-1α* inhibition with *YC-1* significantly decreased cells' migration and capillary forming ability evoked by high-glucose and *NLRP3*, which manifested as more remaining scratch area and fewer junctions, branches, and shorter branching length in the HG+ pcDNA3-N-Flag*NLRP3*+*YC-1* group as compared to

those in the HG+ pcDNA3-N-Flag*NLRP3* group ( $**p<0.01$ ) (Figure 4H–L).

## Discussion

Inflammation and neoangiogenesis are the two main parts of DR. Lots of work has been done on each of them individually, while studies on their interactions are rare. In the present study, our in vivo experiments showed that silencing *NLRP3* could alleviate the histopathological changes in the retinas of DM rats. This was probably because down-regulation of *NLRP3* reduced secretion of pro-inflammatory cytokines and *VEGF*, the levels of which were positively correlated. Further, we identified that the *NLRP3* inflammasome may take part in the neo-vascularization by promoting the expression of *VEGF* in a *HIF-1α* dependent way. In brief, we highlight a protective role of the *NLRP3* blockade in the in vivo

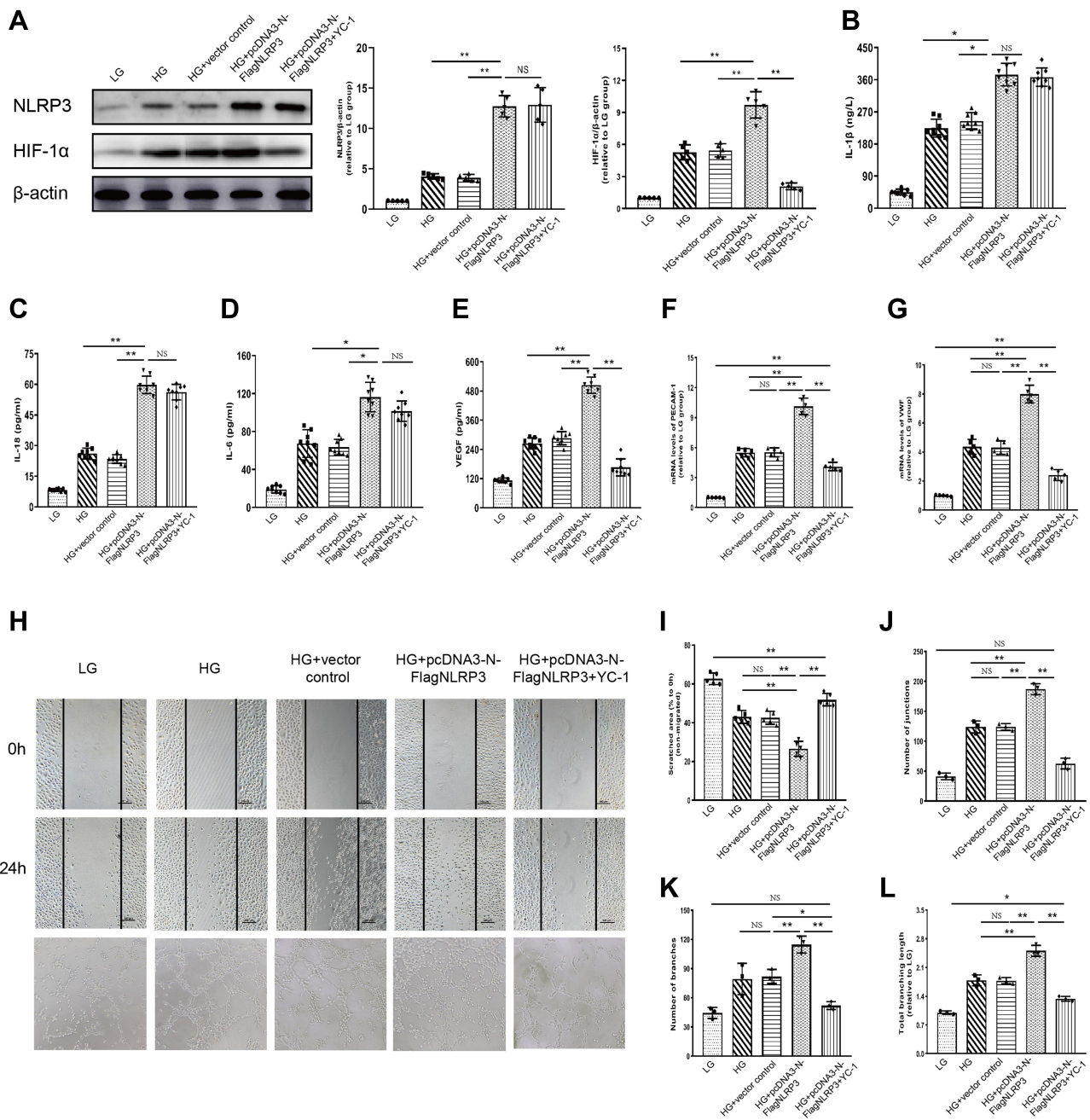


**Figure 4** NLRP3 over-expression promotes secretion of pro-inflammatory and pro-angiogenic cytokines in HRECs cultured in high-glucose media and HIF-1 $\alpha$  inhibitor can reverse NLRP3-induced VEGF production. **(A)** The Western blot assay proved that transfection with NLRP3 over-expressing plasmid could stimulate the expression of NLRP3 as well as of HIF-1 $\alpha$  in HRECs. The NLRP3 induced HIF-1 $\alpha$  expression was reversed by HIF-1 $\alpha$  inhibitor (YC-1) ( $*p < 0.05$ ;  $**p < 0.01$ ; NS: no statistically significant). **(B–D)** Elevated levels of pro-inflammatory IL-1 $\beta$ , IL-18, and IL-6 were observed in the HG and HG+ vector control group compared with the LG group. NLRP3 over-expressing plasmid further increased these elevations, which were not affected by HIF-1 $\alpha$  inhibitor (YC-1) ( $*p < 0.05$ ;  $**p < 0.01$ ; NS: no statistically significant). **(E–G)** High-glucose condition could stimulate the expressions of HIF-1 $\alpha$ , VEGF, PECAM-1 and VWF in HRECs. This stimulatory effect was significantly enhanced in the presence of NLRP3 over-expressing plasmid, which mainly manifested as elevated expressions of HIF-1 $\alpha$ , VEGF, PECAM-1 and VWF in the HG+ pcDNA3-N-FlagNLRP3 group in contrast to the HG and HG+vector control group ( $**p < 0.01$ ). These NLRP3 induced excessive expressions of VEGF, PECAM-1 and VWF was inhibited by HIF-1 $\alpha$  inhibitor (YC-1) ( $**p < 0.01$ ). **(H–L)** High-glucose condition could stimulate cells' migration and capillary forming ability, which was significantly enhanced in the presence of NLRP3 over-expressing plasmid. HIF-1 $\alpha$  inhibition with YC-1 significantly decreased cells' migration and capillary forming ability evoked by high-glucose and NLRP3, which manifested as more remaining scratch area and fewer junctions, branches and shorter branching length in the HG+ pcDNA3-N-FlagNLRP3+YC-1 group as compared to those in the HG+ pcDNA3-N-FlagNLRP3 group ( $**p < 0.01$ ). ( $\times 100$  magnification for scratches and  $\times 200$  magnification for tube formation assay) Data are expressed as mean  $\pm$  SD,  $n = 5$  technical replicates for **(B–E)** and  $n = 8$  technical replicates for **(F–L)**. ( $*p < 0.05$ ;  $**p < 0.01$ ; NS: no statistically significant)

**Abbreviations:** HRECs, human retinal endothelial cells; HIF-1 $\alpha$ , hypoxia inducible factor-1 $\alpha$ ; VEGF, vascular endothelial growth factor; NLRP3, NLR family pyrin domain containing 3; YC-1, (5-(1-benzyl-1H-indazol-3-yl) furan-2-yl)methanol; IL-1 $\beta$ , interleukin-1 $\beta$ ; IL-18, interleukin-18; IL-6, interleukin-6; HG, high glucose; LG, low glucose.

rat model of DR. Down-regulation of NLRP3 suppressed not only inflammatory cytokines but also pro-angiogenic VEGF, indicating that the activated NLRP3 inflammasome may participate in the interlink between inflammation and neovascularization.

Excessive activation of the NLRP3 inflammasome has been observed in many ocular diseases, including eye infections, xerophthalmia, acute glaucoma, and DR. As regards DR, the NLRP3 inflammasome was reported highly expressed in human DR patients' retinal proliferative membranes obtained from surgical resection.<sup>19</sup> In animal models of DR, up-regulation of NLRP3 expression was also observed in the retinas of STZ-induced diabetic mice and rats.<sup>20,21</sup> Similarly, we also confirmed the over-expression of the NLRP3 inflammasome in the retinas of diabetic rats and HRECs cultured in high-glucose media in our study. Previous studies proved that sulforaphane and fenofibrate could attenuate DR and inhibited NLRP3 inflammasome activation.<sup>20,21</sup> However, the effect of specific NLRP3 inflammasome inhibition has still not been defined in the in vivo model of DR. Our research discovered that intravitreal injection of specific shNLRP3 once every four weeks, three times in total, markedly reduced the expression and activation of the NLRP3 inflammasome in diabetic rats' retinas. In addition, it is noteworthy that this specific NLRP3 blockade protected the retinas from morphological changes in the diabetic rats in our study. The diabetic rats treated with specific shRNA-NLRP3 showed greater retinal thickness, better cell arrangement in the INL and ONL, and more ganglion cells in the GCL (Figure 1A–E).

To explore the potential mechanism of the protection provided by specific shNLRP3, we detected several classic pro-inflammatory and pro-angiogenesis cytokines in DR. The priming role of the NLRP3 inflammasome in inflammation has been well established in many diseases. In the field of hyperglycemia-induced injury, Hu et al observed the synchronous increase of HMGB1, TLR4, NLRP3, IL-1 $\beta$ , and IL-18 in ganglion cells treated with different concentrations of glucose.<sup>22</sup> Consistently, we observed the same trend of changes between NLRP3 and inflammatory cytokines such as IL-1 $\beta$ , IL-18, TNF- $\alpha$ , and IL-6 (Figure 2A–D). These results may be explained by the fact that NLRP3 inflammasome activation in the retina enhanced the inflammatory response. This is supported by the fact that the mRNA and protein levels of ASC, caspase-1, and IL-1 $\beta$  decreased when we silenced NLRP3 (Figure 3A–C) and their expression increased in HRECs when NLRP3

was over-expressed (Figure 4B–D). As the main products of NLRP3 inflammasome activation, IL-1 $\beta$  and IL-18 levels decreased significantly in the condition of NLRP3 inhibition. Similar results have also been obtained in many previous studies. Sun J et al discovered that IL- $\beta$  could induce secretion of IL-6 in mesenchymal stem cells.<sup>23</sup> Here, we also found a decreased level of IL-6 in the NLRP3 inhibition group in accordance with the decrease of IL- $\beta$  (Figure 2C). IL-1 $\beta$  stimulated ICAM-1 production has also been reported in ARPE-19 cells.<sup>24</sup> Thus, the reduced level of sICAM-1 in the DM+shNLRP3 group may be partially attributed to the reduction of IL-1 $\beta$  in our study. In addition, it seems that the treatment with the specific shRNA showed levels very comparable to the normal animals for the histomorphometric parameters (Figure 1). In contrast, the cytokine levels were significantly reduced but still very elevated compared to the normal animals (Figure 2). Since we know that morphological and histological changes of retinas usually occur a period of time after the elevation of inflammatory factors, we speculate that this may be because the NLRP3 blockade delayed the secretion and reduced the levels of pro-inflammatory cytokines. Thus, the strength and function time of elevated pro-inflammatory cytokines may not be enough to induce morphological changes. These can be clarified by multi-time point measurements of the cytokine levels during the entire duration in future studies.

The most interesting aspect was that we saw a positive correlation between inflammatory factors (IL-1 $\beta$  and IL-6) and VEGF when *NLRP3* was inhibited (Figure 2G, H). Activation of NLRP3 inflammasome was reported to be involved in VEGF expression under the condition of oxygen-induced retinopathy.<sup>25</sup> Doktor et al suggested that hypoxia caused a synchronous increase of NLRP3 and VEGF expressions in retinal pigment epithelial cells.<sup>26</sup> Sui et al revealed that inhibiting the activity of NLRP3 inflammasome by an antagonist of integrin  $\alpha 5\beta 1$  ameliorated retinal neovascularization induced by VEGF.<sup>27</sup> Nevertheless, the role of NLRP3 inflammasome in the expression of VEGF has still not been elucidated in DR. Our results showed that activated NLRP3 inflammasome may influence both inflammatory cytokines and VEGF, which contribute to their positive correlation.

Regarding the interlink between inflammation and angiogenesis in DR, cyclooxygenase-2, ICAM-1, or CD18 were considered to be the possible crossing points. This is because inhibiting their expression led to obvious alleviation of neovascularization in DR.<sup>28</sup> As an important part of the innate

immune inflammatory response, NLRP3 was recently reported to take part in neovascularization in DR.<sup>14</sup> In the Akimba mouse, over-activation of the NLRP3 inflammasome caused the destruction of the blood–retina barrier as well as vascular leakage due to activation of the micro- and macro-glial cells. Our study showed that rats treated with shNLRP3 had relatively low levels of interleukins and VEGF as well as less retinal damage. Considering its pro-inflammatory features, we identified that the NLRP3 inflammasome may be a potential novel cross point between inflammation and angiogenesis in DR. Further, HRECs were used to explore the underlying mechanism of the NLRP3 inflammasome based on the fact that HREC is one of the main sources of VEGF.<sup>29</sup> Zhang et al found that HIF-1 $\alpha$  was critical for VEGF expression and angiogenesis in DR.<sup>30</sup> In our study, inhibiting activation of the NLRP3 inflammasome reduced expressions of HIF-1 $\alpha$  and VEGF in HRECs. We also identified the decisive role of HIF-1 $\alpha$  in the promotion of VEGF by the NLRP3 inflammasome, given that HIF-1 $\alpha$  inhibitor decreased the production of VEGF induced by over-expressed NLRP3. Therefore, the possible mechanism of the interlink lies in the NLRP3 inflammasome providing a molecular platform for inflammatory cytokines and directly regulating the HIF-1 $\alpha$ /VEGF axis (Figure 5). Previously, HIF-1 $\alpha$  inhibitor has been reported to down-regulate the secretion of IL-6 in the retinas of STZ-induced diabetic rats.<sup>31</sup> In the present study, inhibiting HIF-1 $\alpha$  with

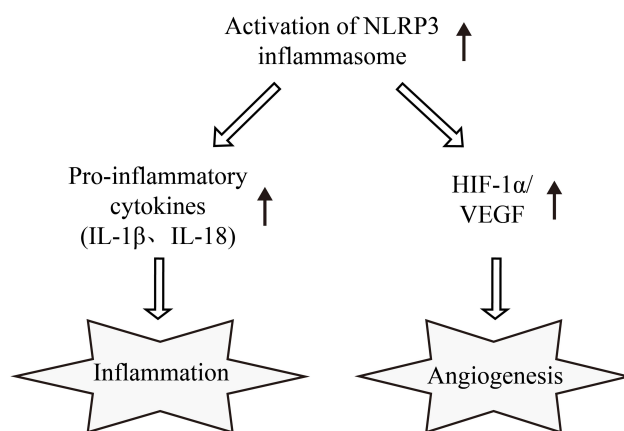


**Figure 5** NLRP3 inflammasome interlinks inflammation and pro-angiogenesis in DR. Based on the results of our study, we presume NLRP3 participates in the interaction between inflammation and pro-angiogenesis in DR. Activated NLRP3 inflammasome provides a molecular platform for the maturation of IL-1 $\beta$  and IL-18 and thus inducing inflammation. Meanwhile, activated NLRP3 inflammasome can promote pro-angiogenic cytokines secretion by up-regulating the HIF-1 $\alpha$ /VEGF axis in HRECs.

**Abbreviations:** NLRP3, NLR family pyrin domain containing 3; DR, diabetic retinopathy; IL-1 $\beta$ , interleukin-1 $\beta$ ; IL-18, interleukin-18; HIF-1 $\alpha$ , hypoxia inducible factor-1 $\alpha$ ; VEGF, vascular endothelial growth factor; HRECs, human retinal capillary endothelial cells.

YC-1 caused a slight reduction of IL-6 induced by NLRP3 over-expression, but the decrease was not statistically significant (Figure 4D). Further studies are needed to investigate the interaction between HIF-1 $\alpha$  and IL-6 in the complex network between inflammation and angiogenesis.

Considering that the main concern of this manuscript is the interlink between the pro-inflammatory and pro-angiogenic role of the NLRP3 inflammasome, and the shRNA we used here did not target a particular cell type, we did not pay much attention to the cell location of NLRP3 reduction in the in vivo experiment in this study. Future studies may bridge this gap by fluorescent localization of the NLRP3 reduction.

All in all, our results confirm the pro-inflammatory and proangiogenic role of NLRP3 inflammasome activation in DR and the effectiveness of shNLRP3 treatment in the in vivo rat model. NLRP3 inflammasome could promote the secretion of pro-inflammatory factors as well as activate the HIF-1 $\alpha$ /VEGF axis, which suggests that future targeted therapy against the NLRP3 inflammasome may have these dual effects.

## Acknowledgment

This work was sponsored by the National Natural Science Foundation of China [grant number 81200718 and 81570866].

## Disclosure

The authors report no conflicts of interest for this work.

## References

- Ogurtsova K, da Rocha Fernandes JD, Huang Y, et al. IDF Diabetes Atlas: global estimates for the prevalence of diabetes for 2015 and 2040. *Diabetes Res Clin Pract.* 2017;128:40–50. doi:10.1016/j.diabres.2017.03.024
- Alves BC, Silva TR, Spritzer PM, Lifestyle S. High-carbohydrate intake are associated with low-grade chronic inflammation in post-menopause: a cross-sectional study. *Rev Bras Ginecol Obstet.* 2016;38(7):317–324. doi:10.1055/s-0036-1584582
- Rubsam A, Parikh S, Fort PE. Role of inflammation in diabetic retinopathy. *Int J Mol Sci.* 2018;19(4):942. doi:10.3390/ijms19040942
- Cai M, Zhang X, Li Y, et al. Toll-like receptor 3 activation drives the inflammatory response in oxygen-induced retinopathy in rats. *Br J Ophthalmol.* 2015;99(1):125–132. doi:10.1136/bjophthalmol-2014-305690
- Liu X, Zhang Z, Ruan J, et al. Inflammasome-activated gasdermin D causes pyroptosis by forming membrane pores. *Nature.* 2016;535(7610):153–158. doi:10.1038/nature18629
- Feng H, Gu J, Gou F, et al. High Glucose and Lipopolysaccharide Prime NLRP3 Inflammasome via ROS/TXNIP pathway in mesangial cells. *J Diabetes Res.* 2016;2016:6973175. doi:10.1155/2016/6973175
- Zhong Z, Umemura A, Sanchez-Lopez E, et al. NF-kappaB restricts inflammasome activation via elimination of damaged mitochondria. *Cell.* 2016;164(5):896–910. doi:10.1016/j.cell.2015.12.057

8. Tartey S, Kanneganti TD. Differential role of the NLRP3 inflammasome in infection and tumorigenesis. *Immunology*. 2019;156(4):329–338. doi:10.1111/imm.13046
9. Malhotra S, Costa C, Eixarch H, et al. NLRP3 inflammasome as prognostic factor and therapeutic target in primary progressive multiple sclerosis patients. *Brain*. 2020;143(5):1414–1430. doi:10.1093/brain/awaa084
10. Minutoli L, Puzzolo D, Rinaldi M, et al. ROS-Mediated NLRP3 inflammasome activation in brain, heart, kidney, and testis ischemia/reperfusion injury. *Oxid Med Cell Longev*. 2016;2016:2183026. doi:10.1155/2016/2183026
11. Chi W, Chen H, Li F, et al. HMGB1 promotes the activation of NLRP3 and caspase-8 inflammasomes via NF-kappaB pathway in acute glaucoma. *J Neuroinflammation*. 2015;12:137. doi:10.1186/s12974-015-0360-2
12. Park B, Jo K, Lee TG, et al. Polydatin Inhibits NLRP3 inflammasome in dry eye disease by attenuating oxidative stress and inhibiting the NF-kappaB pathway. *Nutrients*. 2019;11(11):2792. doi:10.3390/nu1112792
13. Sun HJ, Jin XM, Xu J, et al. Baicalin alleviates age-related macular degeneration via miR-223/NLRP3-regulated pyroptosis. *Pharmacology*. 2020;105(1–2):28–38. doi:10.1159/000502614
14. Chaurasia SS, Lim RR, Parikh BH, et al. The NLRP3 inflammasome may contribute to pathologic neovascularization in the advanced stages of diabetic retinopathy. *Sci Rep*. 2018;8(1):2847. doi:10.1038/s41598-018-21198-z
15. Shi H, Zhang Z, Wang X, et al. Inhibition of autophagy induces IL-1 $\beta$  release from ARPE-19 cells via ROS mediated NLRP3 inflammasome activation under high glucose stress. *Biochem Biophys Res Commun*. 2015;463(4):1071–1076. doi:10.1016/j.bbrc.2015.06.060
16. Jiang Y, Liu L, Curtiss E, et al. Epac1 Blocks NLRP3 Inflammasome to Reduce IL-1 $\beta$  in retinal endothelial cells and mouse retinal vasculature. *Mediators Inflamm*. 2017;2017:2860956. doi:10.1155/2017/2860956
17. Jiang S, Chen X. HMGB1 siRNA can reduce damage to retinal cells induced by high glucose in vitro and in vivo. *Drug Des Devel Ther*. 2017;11:783–795. doi:10.2147/DDDT.S129913
18. Wu J, Ke X, Fu W, et al. Inhibition of hypoxia-induced retinal angiogenesis by specnuezhenide, an effective constituent of ligustrum lucidum ait., through suppression of the HIF-1 $\alpha$ /VEGF signaling pathway. *Molecules*. 2016;21(12). doi:10.3390/molecules21121756
19. Zhang Y, Lv X, Hu Z, et al. Protection of Mcc950 against high-glucose-induced human retinal endothelial cell dysfunction. *Cell Death Dis*. 2017;8(7):e2941. doi:10.1038/cddis.2017.308
20. Liu Q, Zhang F, Zhang X, et al. Fenofibrate ameliorates diabetic retinopathy by modulating Nrf2 signaling and NLRP3 inflammasome activation. *Mol Cell Biochem*. 2018;445(1–2):105–115. doi:10.1007/s11010-017-3256-x
21. Li S, Yang H, Chen X. Protective effects of sulforaphane on diabetic retinopathy: activation of the Nrf2 pathway and inhibition of NLRP3 inflammasome formation. *Exp Anim*. 2019;68(2):221–231. doi:10.1538/expanim.18-0146
22. Hu L, Yang H, Ai M, et al. Inhibition of TLR4 alleviates the inflammation and apoptosis of retinal ganglion cells in high glucose. *Graefes Arch Clin Exp Ophthalmol*. 2017;255(11):2199–2210. doi:10.1007/s00417-017-3772-0
23. Sun J, Liao W, Su K, et al. Suberoylanilide hydroxamic acid attenuates interleukin-1 $\beta$ -induced interleukin-6 upregulation by inhibiting the microtubule affinity-regulating kinase 4/nuclear Factor-kappaB pathway in synovium-derived mesenchymal stem cells from the temporomandibular joint. *Inflammation*. 2020. doi:10.1007/s10753-020-01204-1
24. Cheng SC, Huang WC, SP JH, et al. Quercetin Inhibits the Production of IL-1 $\beta$ -induced inflammatory cytokines and chemokines in ARPE-19 Cells via the MAPK and NF-kappaB signaling pathways. *Int J Mol Sci*. 2019;20:12. doi:10.3390/ijms20122957
25. Wang S, Ji L-Y, Li L, et al. Oxidative stress, autophagy and pyroptosis in the neovascularization of oxygen-induced retinopathy in mice. *Mol Med Rep*. 2019;19(2):927–934. doi:10.3892/mmr.2018.9759
26. Doktor F, Prager P, Wiedemann P, et al. Hypoxic expression of NLRP3 and VEGF in cultured retinal pigment epithelial cells: contribution of P2Y2 receptor signaling. *Purinergic Signal*. 2018;14(4):471–484. doi:10.1007/s11302-018-9631-6
27. Sui A, Zhong Y, Demetriades AM, et al. Inhibition of integrin alpha5beta1 ameliorates VEGF-induced retinal neovascularization and leakage by suppressing NLRP3 inflammasome signaling in a mouse model. *Graefes Arch Clin Exp Ophthalmol*. 2018;256(5):951–961. doi:10.1007/s00417-018-3940-x
28. Ayalasomayajula SP, Kompella UB. Celecoxib, a selective cyclooxygenase-2 inhibitor, inhibits retinal vascular endothelial growth factor expression and vascular leakage in a streptozotocin-induced diabetic rat model. *Eur J Pharmacol*. 2003;458(3):283–289. doi:10.1016/s0014-2999(02)02793-0
29. Xu XH, Zhao C, Peng Q, et al. Kaempferol inhibited VEGF and PGF expression and in vitro angiogenesis of HRECs under diabetic-like environment. *Braz J Med Biol Res*. 2017;50(3):e5396. doi:10.1590/1414-431X20165396
30. Zhang D, Lv FL, Wang GH. Effects of HIF-1 $\alpha$  on diabetic retinopathy angiogenesis and VEGF expression. *Eur Rev Med Pharmacol Sci*. 2018;22(16):5071–5076. doi:10.26355/eurrev\_201808\_15699
31. Gao X, Li Y, Wang H, et al. Inhibition of HIF-1 $\alpha$  decreases expression of pro-inflammatory IL-6 and TNF- $\alpha$  in diabetic retinopathy. *Acta Ophthalmol*. 2017;95(8):e746–e50. doi:10.1111/aos.13096

## Diabetes, Metabolic Syndrome and Obesity: Targets and Therapy

Dovepress

### Publish your work in this journal

Diabetes, Metabolic Syndrome and Obesity: Targets and Therapy is an international, peer-reviewed open-access journal committed to the rapid publication of the latest laboratory and clinical findings in the fields of diabetes, metabolic syndrome and obesity research. Original research, review, case reports, hypothesis formation, expert opinion

and commentaries are all considered for publication. The manuscript management system is completely online and includes a very quick and fair peer-review system, which is all easy to use. Visit <http://www.dovepress.com/testimonials.php> to read real quotes from published authors.

Submit your manuscript here: <https://www.dovepress.com/diabetes-metabolic-syndrome-and-obesity-targets-and-therapy-journal>